

EFFECT OF ELASTIC BEND DISTORTIONS ON ELECTRON DIFFRACTION DATA FROM THIN PROTEIN MICROCRYSTALS

Douglas L. DORSET

Electron Diffraction Department, Medical Foundation of Buffalo, Inc., 73 High Street, Buffalo, New York 14203, USA

Received 25 October 1985; received in final form 6 June 1986

The effect of small elastic bend distortions in thin protein crystals on electron diffraction intensities is investigated using a model calculation for rubredoxin. The calculation, based on analytical expression derived by Cowley, has been shown previously to give an almost quantitative description of kinematical diffraction from linear chain systems. It is therefore shown that, unless the selected area used in the electron diffraction experiment is very small (or alternatively the incident beam has a small coherence length), the high resolution data may not be useful for structure determination, since they do not represent the total contents of the unit cell.

1. Introduction

For macromolecules which are most easily prepared as microcrystalline samples, the use of electron crystallographic techniques has proved to be successful for quantitative structure determination at moderate resolutions (e.g. 20–7 Å), giving some insights into the molecular shapes and aggregations of a wide variety of substances including integral membrane proteins, globular proteins and ribonucleic acids. Considerable effort has been spent to devise sophisticated image processing systems in order to extract the most representative average structure from the sample. In an attempt to overcome the constraints imposed by solvent loss, various embedding media (including sugars and vitreous ice) have been used, replacing traditional negative stains, giving an added benefit of enhanced structure preservation to at least the 3 Å observed in many electron diffraction patterns from such specimens. It seems that at room temperature electron-beam-induced radiation damage limits the direct structural interpretation of images to about 7 Å [1], beyond which it is hoped that some phase extension technique would allow resolution enhancement to the limits set by the electron diffraction data.

Although many possible perturbations to image

and diffraction data have been investigated, rather basic ones which result from the fundamental scattering properties of the sample have been largely overlooked. For example, in the analysis of electron microscope data from such crystals it is commonly assumed that the thin phase object approximation is correct, even for negatively stained preparations. Only recently has this problem been realistically evaluated in three dimensions [2] via multislice *n*-beam dynamical calculations of the projected lattice potential using the phase gratings $q(x, y)$ from successive slices through the crystal, i.e.

$$q(x, y) = \exp[-i\sigma\rho(x, y) - \mu(x, y)],$$

which include the projected slice potential $\rho(x, y)$ and allow for an “absorption” term $\mu(x, y)$. At 20 Å resolution it was shown that the mass distribution and symmetry of the projected structure could be trusted to perhaps a 500 Å crystal thickness for an object lightly stained with uranyl acetate. Multislice calculations have also been carried out for an unstained protein [3].

In molecular crystals, another significant perturbation to diffracted intensity is the effect of lattice bend distortions, particularly if the projected unit cell axis is large [4–9]. While it is possible to epitaxially recrystallize oblong mole-

cules to place a shorter unit cell axis in the beam direction [10], such a remedy is not possible for proteins which crystallize with large unit cell axes in every direction. Since these bend distortions affect high-angle diffraction data most markedly so that they may no longer represent the total contents of the unit cell, it is important to evaluate their effect on protein data, particularly if high resolution information from experimental electron diffraction intensities is anticipated. Another aspect of bending, i.e. the smearing of electron diffraction peaks for high tilt data, has already been discussed [11,12].

2. Model calculation

Using the crystal bending model of Cowley [13], the elastic distortion of a crystalline film is simulated by a Gaussian term which modulates the unit cell Patterson function as it is Fourier transformed to give the diffracted intensities for a zone of reflections. In the analytical expression for the intensity of a reflection at reciprocal lattice vector s ,

$$I(s) = \sum_i W_i(s) \exp(2\pi i \mathbf{r}_i \cdot \mathbf{s}) \exp(-\pi^2 c^2 s^2 z_i^2), \quad (1)$$

the form factor W_i of Patterson vector i is altered according to the magnitude of crystal bend c (in radians), the magnitude $s = |\mathbf{s}|$ of the reciprocal vector and the component of the Patterson vector z_i along the beam axis. It is readily seen that beyond $z_i = 1/\pi cs$ for Patterson vector i , then, this contribution to the intensity becomes very small. This model has been found to be remarkably quantitative for explaining the experimental electron diffraction from n-paraffins [4,5], phospholipids [9], cholesteryl esters [14] and linear polymers [7] in a projection down the long molecular axis, even though it assumes the crystals to be regularly bent. The theoretical justification for this approximation at small bends has been given from n-beam dynamical calculations for curved crystals [8], since, in principle, the two effects cannot be separated unless one dominates over the other. In this model, a coherent source is assumed, as is

provided by the lens arrangements often used for low-dose electron diffraction experiments [15].

Since its crystal structure is known to 1.5 Å resolution, the molecular packing of rubredoxin [16] was used for model calculations. The crystal structure has space group symmetry R3 (C_3^4 , No. 146 [17]) with unit cell parameters $a = 38.77$ Å, $\alpha = 112.37^\circ$. There are three molecules per unit cell. Although it is relatively easy to write a computer program to calculate intensities according to (1) (we use a program written by Dr. Barbara Moss), the formidable number of atoms in a protein crystal structure generate a larger ($N^2 - N + 1$) number of Patterson terms which may not be easily accommodated on many computers (while using standard programs for Fourier transforms) such that the computation will proceed in a reasonable amount of time. Excluding solvent molecules, there are some 426 atoms in the rubredoxin structure, generating 1.81×10^5 non-origin Patterson peaks for the asymmetric unit or 1.63×10^6 for the unit cell. In this calculation we have decided to use only the 218 chain backbone atoms as well as an iron position (assigning an average isotropic temperature factor $B = 15$ Å² for all atoms). This will give 4.77×10^4 autocorrelation peaks or 4.31×10^5 peaks in the rhombohedral unit cell. The hexagonal unit cell atomic coordinates for rubredoxin were transformed to the rhombohedral cell coordinates with the required transformation matrix given in Volume I of the International Tables for X-Ray Crystallography [17]. These kinematical calculations are carried out to a 3 Å resolution, simulating the electron diffraction limit often found for suitably preserved protein microcrystals. The 38.8 Å projection distance for calculations of $hk0$ intensities is something of an underestimate for typical protein unit cell thicknesses.

3. Results

Calculated structure factor moduli for various bend values within the range found from bend contours on molecular crystals [4] were compared to moduli from an unbent structure. These are presented in fig. 1 as plots of crystallographic

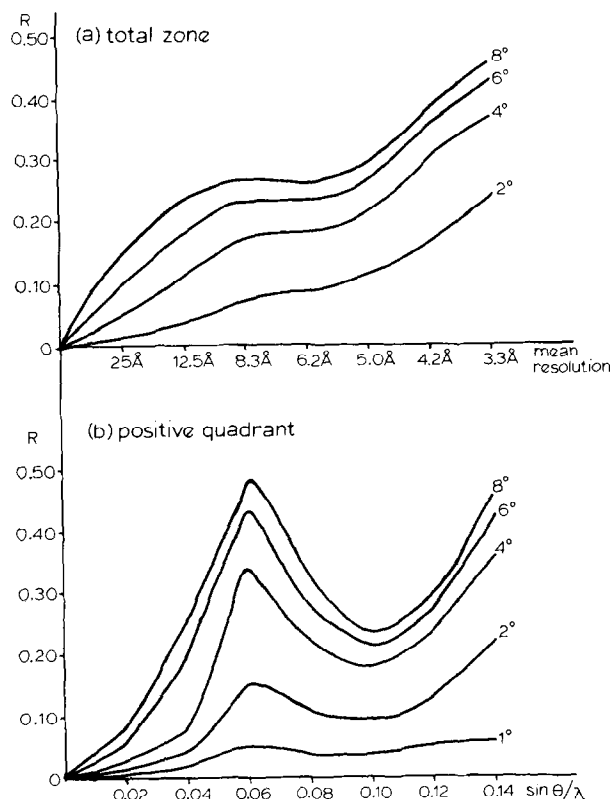


Fig. 1. Plots of crystallographic residuals for overlapping shells of reciprocal lattice points comparing structure factor magnitudes of an unbent rubredoxin crystal to those for various values of crystal bend. The projection is down [100]. (a) Comparison of complete $hk0$ data sets; (b) comparison of data sets where h and k are both positive.

residuals:

$$R = \frac{\sum_{hk} |F_{\text{unbent}}^{hk}| - |F_{\text{bent}}^{hk}|}{\sum_{hk} |F_{\text{unbent}}^{hk}|}, \quad (2)$$

for overlapping zones in $(\sin \theta)/\lambda$ with width 0.04 \AA^{-1} . Two types of data are used for this comparison. For the total zonal data, the increasing disagreement between diffraction data from bent and unbent crystals almost seems to follow a regular curve. The data sample from a quadrant with only all positive Miller indices, on the other hand, reveals the structural specificity of this bend phenomenon, since two R value minima are observed.

Another aspect of the bend distortion is that

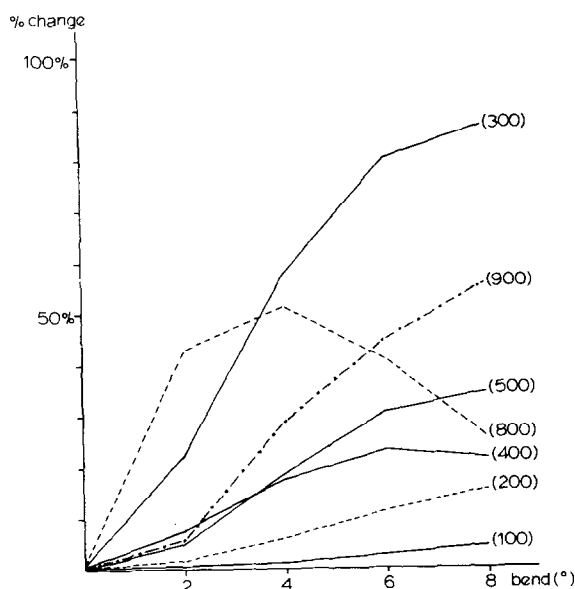


Fig. 2. Percentage change $|\Delta F_{hk}/F_{hk}|$ of structure factor magnitudes for axial reflections F_{h0} compared to R3 symmetrically related F_{0h} . The deviation from R3 symmetry is clearly shown, especially for higher-angle reflections.

the symmetry of the unit cell projection is changed, as originally found by Cowley [13] in his study of silicates. For rubredoxin this can be most easily visualized by comparing the percentage change of reflection intensities which should be equivalent by R3 symmetry, i.e. for the $hk0$ data the magnitudes $|F_{h00}| \equiv |F_{0h0}|$ in the unbent crystal. With bending the values $|\Delta F|/|F_{\text{unbent}}|$, where $\Delta F = ||F_{h00}| - |F_{0h0}||$, plotted in fig. 2 are seen to change in an irregular fashion. The least change is seen for low angle data, as expected, but higher resolution data are changed in a way that is dependent on the structure projection as also found strikingly for oblique layer molecular crystals [4]. The absence of a well-oriented regular sublattice (which can be found for polymethylene compounds), moreover, means that no invariant structure projection can be found here.

4. Discussion

The relevance of the foregoing model calculation depends on at least four factors, viz:

- (a) the actual coherence length of the electron source (Young's fringe experiment);
- (b) the diameter of the illuminated area on the specimen;
- (c) the length of the projected unit cell axis in the crystalline sample;
- (d) the amount of crystal bending within a limiting diameter defined by the smaller of (a) or (b).

Theoretical diffraction resolutions for various magnetic lens configurations used for electron diffraction have been compiled by Ferrier [15]. At 80 kV, the resolution for selected area diffraction is ca. 1.0 μm ; the resolution for the low-angle diffraction mode often used in protein electron crystallography (Bassett-Keller method [19]) is ca. 0.5 μm . As stated by Ferrier, the coherence length of the electron source is greater or equal to the diffraction coherence. For example, in an illustrated low-angle electron diffraction pattern from a 0.463 μm repeat grating standard [15], a shape transform broadening is seen which corresponds to about two grating repeats. Thus, although the theoretical diffraction resolution for this mode (not the Bassett-Keller method already mentioned), defined by the angular resolution α is

$$d_{\text{max}} = \lambda/\alpha = 4.177 \times 10^{-2} \text{ \AA} / 4 \times 10^{-6} = 1.0 \text{ \AA}, \quad (3)$$

the coherence length is twice this value. Such coherence lengths are much greater than those found for typical X-ray sources. This is why particular attention must be paid to the coherent electron diffraction from a curved specimen, even though the X-ray diffraction from the same specimen could be treated adequately by a mosaic crystal model.

If the beam coherence length is defined by the electron microscope configuration used for electron diffraction, then the illuminated area on the specimen can be minimized by the limiting aperture diameter (e.g. the second condenser aperture for the Bassett-Keller method). For example, Baldwin and Henderson [11] cite a 0.2 μm sampled diameter in their diffraction work on bacteriorhodopsin. Aside from these instrumental factors, other considerations for evaluating the importance of eq. (1) depend on specimen parameters.

It is therefore necessary to be constantly aware that electron diffraction structure analysis is not the same thing as X-ray crystallographic analysis and that certain conditions must be satisfied to permit an *ab initio* structure analysis to be carried out. If the limiting factors discussed above are ignored, then a high resolution phase extension based solely on the diffraction intensities may be meaningless because these intensities no longer represent the Fourier transform of the total unit cell Patterson function. Crystal curvature has significantly influenced the structure analysis of the molecular crystals [4–9] and, in some cases, has prompted the use of alternative crystallization techniques to produce a more favorable structure projection. In other cases, adequate structure refinement was possible only after the crystal bending was incorporated into the model [7].

5. Conclusions

Bend deformation of thin crystals is a universal constraint in electron microscopy. Since proteins have very large unit cell axes (as do lipids in one direction), the use of electron diffraction data may be unreliable at high resolution due to the effective diffraction incoherence imposed by the bend deformation. Since there is no substructure in these materials (unlike lipids which have a shorter subcell repeat which can provide at least some structural information), the use of electron diffraction data for phase extension at high resolutions must be done only with specimens for which the sampled curvature within the coherence length (or aperture limitation) is very small.

Acknowledgements

This work could not have been done without the friendly support of the electron microscopy department at the Fritz-Haber-Institut in Berlin/Dahlem who permitted me to use the VAX 11/780 computer which had quite adequate disc space for this calculation. Special thanks are given to Professor Elmar Zeitler and Dr. Marin van Heel for their cooperation and assistance. This

work was partly funded also by grant GM21047 from the National Institute of General Medical Sciences.

References

- [1] P.N.T. Unwin and R. Henderson, *J. Mol. Biol.* 94 (1975) 425.
- [2] D.L. Dorset, *Ultramicroscopy* 13 (1984) 311.
- [3] M.-S. Ho, B.K. Jap and R.M. Glaeser, in: *Proc. 37th Annual EMSA Meeting*, San Antonio, TX, 1979, Ed. G.W. Bailey (Claitor's, Baton Rouge, LA, 1979) p. 118.
- [4] D.L. Dorset, *Z. Naturforsch.* 33a (1978) 964.
- [5] D.L. Dorset, *Acta Cryst.* A36 (1980) 592.
- [6] B. Moss and D.L. Dorset, *Acta Cryst.*, A38 (1982) 207.
- [7] B. Moss and D.L. Dorset, *J. Polymer Sci. Polymer Phys. Ed.* 20 (1982) 1789.
- [8] B. Moss and D.L. Dorset, *Acta Cryst. A* 39 (1983) 609.
- [9] D.L. Dorset, *Ultramicroscopy* 12 (1983) 19.
- [10] J.C. Wittmann and B. Lotz, in: *Electron Microscopy and Analysis 1985*, *Inst. Phys. Conf. Ser.* 78, Ed. G.J. Tatlock (Inst. Phys., London-Bristol, 1986).
- [11] J. Baldwin and R. Henderson, *Ultramicroscopy* 14 (1984) 319.
- [12] R.M. Glaeser, *Ann. Rev. Phys. Chem.* 36 (1985) 243.
- [13] J.M. Cowley, *Acta Cryst.* 14 (1961) 920.
- [14] D.L. Dorset, *J. Lipid Res.* 26 (1985) 1142.
- [15] R.P. Ferrier, *Advan. Opt. Electron Microsc.* 3 (1969) 155.
- [16] K.D. Watenpaugh, L.C. Sieker, J.R. Herriott and L.H. Jensen, *Acta Cryst.* B29 (1973) 943.
- [17] *International Tables for X-Ray Crystallography*, Vol. 1, Symmetry Groups, Eds. N.F.M. Henry and K. Lonsdale (Kynoch, Birmingham, 1969).
- [18] A. Engel, A. Massalski, D.L. Dorset and J.P. Rosenbusch, *Nature* 317 (1985) 643.
- [19] G.A. Bassett and A. Keller, *Phil. Mag.* 9 (1964) 817.